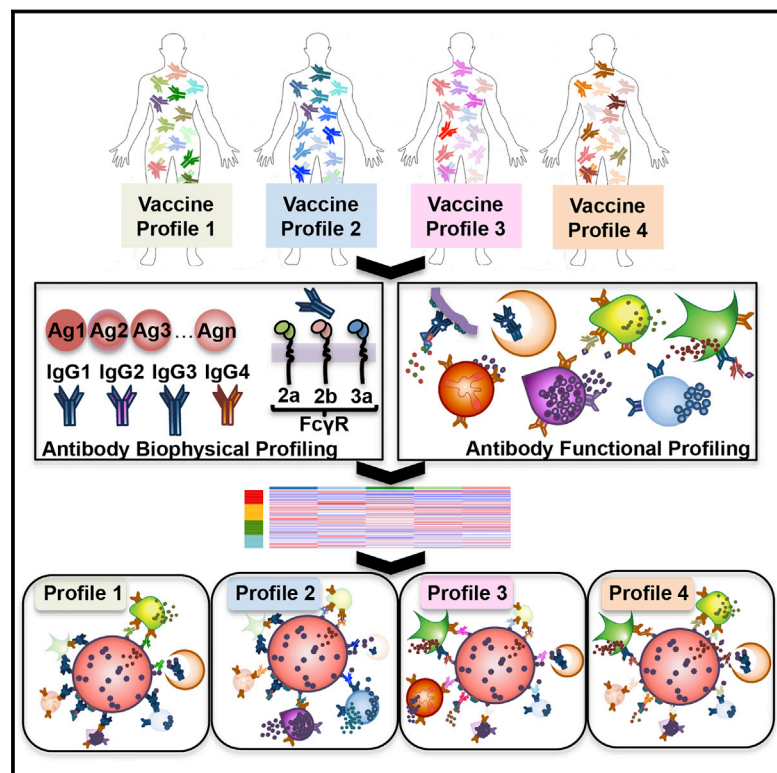Article

Dissecting Polyclonal Vaccine-Induced Humoral Immunity against HIV Using Systems Serology

Graphical Abstract

Authors

Amy W. Chung, Manu P. Kumar, Kelly B. Arnold, ..., Dan H. Barouch, Douglas A. Lauffenburger, Galit Alter

Correspondence

lauffen@mit.edu (D.A.L.), galter@mgh.harvard.edu (G.A.)

In Brief

Systems Serology reveals unique vaccine-induced "fingerprints," highlighting potential markers of protection against HIV and providing a powerful method for comparing candidate vaccines against pathogens for which correlates of protection remain elusive.

Highlights

- Beyond neutralization, antibodies drive antiviral control via Fc-mediated functions

- Distinct vaccines elicit unique antibody Fc-effector profiles

- Network analyses comprehensively integrating antibody profiles can compare vaccines

- Case:control RV144 analysis points to mechanisms of reduced risk of HIV infection

CrossMark

CellPress

Dissecting Polyclonal Vaccine-Induced Humoral Immunity against HIV Using Systems Serology

Amy W. Chung,[1,2,12] Manu P. Kumar,[3,12] Kelly B. Arnold,[3,12] Wen Han Yu,[1,3,12] Matthew K. Schoen,[1] Laura J. Dunphy,[3] Todd J. Suscovich,[1] Nicole Frahm,[4] Caitlyn Linde,[1] Alison E. Mahan,[1] Michelle Hoffner,[1] Hendrik Streeck,[5,6] Margaret E. Ackerman,[7] M. Juliana McElrath,[4] Hanneke Schuitemaker,[8] Maria G. Pau,[8] Lindsey R. Baden,[1,9] Jerome H. Kim,[5,10] Nelson L. Michael,[5] Dan H. Barouch,[1,11] Douglas A. Lauffenburger,[3,*] and Galit Alter[1,*]

[1]Ragon Institute of MGH, MIT, and Harvard, Cambridge, MA 02139, USA
[2]Department of Microbiology and Immunology, Peter Doherty Institute, University of Melbourne, Parkville, VIC 3010, Australia
[3]Department of Biological Engineering, Massachusetts Institute of Technology, Cambridge, MA 02139, USA
[4]Fred Hutchinson Cancer Research Center, Seattle, WA 98109, USA
[5]Department of Molecular Virology and Pathogenesis, Walter Reed Army Institute of Research, U.S. Military HIV Research Program, Silver Spring, MD 20910, USA
[6]Institute for Medical Biology, University Hospital Essen, University Duisburg-Essen, Essen 45141, Germany
[7]Thayer School of Engineering at Dartmouth, Hanover, NH 03755, USA
[8]Crucell Holland B.V., The Janssen Pharmaceutical Companies of Johnson & Johnson, Leiden 2333, the Netherlands
[9]Division of Infectious Diseases, Brigham and Women's Hospital, Boston, MA 02215, USA
[10]International Vaccine Institute, Seoul 151-742, Republic of Korea
[11]Center for Virology and Vaccine Research, Beth Israel Deaconess Medical Center, Harvard Medical School, Boston, MA 02215, USA
[12]Co-first author
*Correspondence: lauffen@mit.edu (D.A.L.), galter@mgh.harvard.edu (G.A.)
http://dx.doi.org/10.1016/j.cell.2015.10.027

SUMMARY

While antibody titers and neutralization are considered the gold standard for the selection of successful vaccines, these parameters are often inadequate predictors of protective immunity. As antibodies mediate an array of extra-neutralizing Fc functions, when neutralization fails to predict protection, investigating Fc-mediated activity may help identify immunological correlates and mechanism(s) of humoral protection. Here, we used an integrative approach termed Systems Serology to analyze relationships among humoral responses elicited in four HIV vaccine trials. Each vaccine regimen induced a unique humoral "Fc fingerprint." Moreover, analysis of case:control data from the first moderately protective HIV vaccine trial, RV144, pointed to mechanistic insights into immune complex composition that may underlie protective immunity to HIV. Thus, multi-dimensional relational comparisons of vaccine humoral fingerprints offer a unique approach for the evaluation and design of novel vaccines against pathogens for which correlates of protection remain elusive.

INTRODUCTION

Although over 80 vaccines, covering more than 20 diseases, have been licensed in the United States, vaccine design efforts against persisting infections, including malaria, tuberculosis, and HIV, continue to fail. These setbacks have driven a shift from empirical vaccine design approaches to rational vaccine development strategies that consider pathogen life cycle, pathogen structural information, and immunological correlates of protection. However, the immune correlates for most globally lethal pathogens have yet to be defined, complicating vaccine design efforts. Prospective immunogens are frequently chosen based on measures of antibody (Ab) titer and neutralization, regardless of their mechanistic effects in immunity. However, for most clinically approved vaccines, titer and neutralization activity alone do not account for protective immunity (Pulendran and Ahmed, 2011). Instead, protective immunity is often observable in the absence of neutralization, and accumulating evidence across a spectrum of vaccines has suggested a critical role for extra-neutralizing Ab functions such as Ab-dependent cellular cytotoxicity (ADCC), Ab-dependent cellular phagocytosis (ADCP), Ab-dependent complement deposition (ADCD), and Ab-dependent respiratory burst (ADRB) in both protection from and post-infection control of HIV (Barouch et al., 2015; Bournazos et al., 2014; Hessell et al., 2007), influenza (DiLillo et al., 2014; Jegerlehner et al., 2004), herpes simplex virus (HSV) (Kohl and Loo, 1982; Kohl et al., 1981), Ebola virus (Warfield et al., 2007), and malaria (Joos et al., 2010; Osier et al., 2014).

Following vaccination, Abs targeting an extensive array of epitopes with different affinities and Fc-effector profiles collectively contribute to the formation of immune complexes that direct antimicrobial functions via their constant domains (Fc). In addition to the rapid diversification of the antigen (Ag)-binding domain (Fab), the Fc domain is also rapidly tuned during an immune response, altering the affinity of Ab interactions with innate immune receptors (e.g., Fc receptors and complement) expressed on all innate immune cells (Ackerman and Alter, 2013; Chung and Alter, 2014). The diversity of Fc profiles, potential Fab variants, and tissue-specific Fc receptor expression results
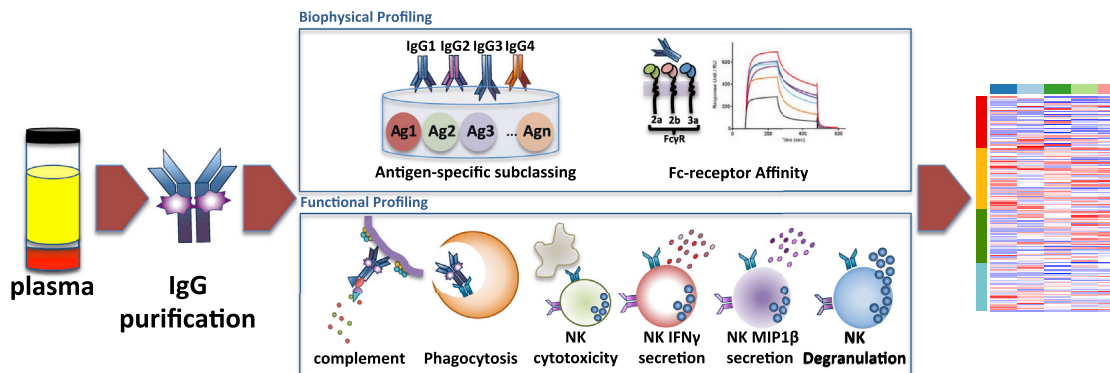
Figure 1. System Serology Analysis
This Systems Serology platform allows for the broad characterization of the polyclonal extra-neutralizing IgG immune profile induced by vaccination. IgG was purified from subjects enrolled in four different HIV vaccine trials (RV144, VAX003, HVTN204, and IPCAVD001). Six Fc-effector functions and 58 biophysical measurements were assayed (complete list described in Table S1). All 64 parameters were collected to create an extra-neutralizing serological signature for the four vaccine trials, using an array of unsupervised and supervised machine learning algorithms.
See also Tables S1 and S2.

in a flexible humoral immune response poised for the elimination of pathogens via mechanisms beyond simple neutralization. Hence, analytical approaches able to integrate diverse facets of the humoral immune response will be critical to: (1) define unexpected correlates of protection from infection in protection studies or studies of natural disease resistance, (2) guide the selection of promising vaccines/immunogens through principled analysis of humoral immune profiles, and (3) define the relationships between Ab populations and functions that point to mechanisms of protective immunity.

As a prominent example, the ability to select HIV vaccine candidates has been hindered by an inadequate understanding of the immunological correlates of protection from HIV. However, several clinical trials have been conducted, one of which (RV144) demonstrated a modest level of protection (31.2% reduction in the risk of infection) (Rerks-Ngarm et al., 2009), potentially harboring clues that may guide future vaccine development. This protection was observed in the absence of neutralizing Abs, cytotoxic T-cell responses, and high Ab titers. Univariate and multivariate logistic regression analyses linked the reduced risk of infection with non-immunoglobulin (Ig)A Ab responses targeting the V1V2 region of the HIV envelope and ADCC activity (Haynes et al., 2012; Zolla-Pazner et al., 2014). Follow-up analyses identified additional features of the humoral immune response associated with protection, including the preferential induction of IgG3 responses, which coordinated multiple Ab effector functions, including ADCC and ADCP (Chung et al., 2014b; Yates et al., 2014). However, in the correlates analysis, although many Ab assays were initially considered, the identification of immune correlates in RV144 was constrained by the selected assays that deeply interrogated neutralization and Ab specificity but profiled only a limited set of Fc features, including only a few Ab subclasses/isotypes (IgG, IgG3, IgA) and a single function, ADCC.

Here, we aimed to consider more integrative and network-oriented relationships between a broader array of polyclonal Ab features and functional properties associated with vaccine

regimens and outcomes. As an initial test of this approach, termed "Systems Serology," we examined recent HIV vaccine trials, including that of the moderately protective RV144 vaccine ALVAC/AIDSVAX B/E (Rerks-Ngarm et al., 2009), two trials that did not demonstrate efficacy in phase 2b trials, (VAX003; AIDSVAX B/E [Pitisuttithum et al., 2006] and HVTN204; DNA/rAD5 [Churchyard et al., 2011]), and one experimental phase 1 study designed to evaluate the prototype vaccine Ad26 vector (IPCAVD001; Ad26.ENVA.01) (Barouch et al., 2013a). A battery of modeling techniques that emphasize co-variation among measurements was applied to these data, revealing features of vaccine–induced "fingerprints" that offer new insights concerning polyclonal Ab immune responses elicited by vaccines.

RESULTS

Systems Serology
Beyond their role in neutralization, Abs mediate a vast array of additional functions via their Fc domains. Thus, a Systems Serology approach was developed to broadly profile the extra-neutralizing Ab activity of vaccine-induced polyclonal Abs (Figure 1). The initial platform interrogated six Fc-effector functions (ADCC, ADCP, ADCD, and three Ab-dependent natural killer (NK) cell activities (Figure 1). Linked to these six functions, 58 biophysical measurements were simultaneously captured, including binding to Fcγ receptors (FCGRs) and the relative abundances of an array of Ag-specific Abs (Table S1) in 120 samples from four HIV vaccine trials (see Supplemental Experimental Procedures).

Identification of Vaccine-Specific Signatures
Unsupervised hierarchical clustering grouped vaccine regimens primarily by immunogen type (Figure 2; Table S2), including an adenovirus (Ad) vector cluster composed of mixed HVTN204 (DNA/Ad5) and IPCAVD001 (Ad26) samples (Figure 2, cluster 1: green and yellow, respectively) and a protein immunogen cluster containing largely mixed VAX003 (protein alone) and RV144
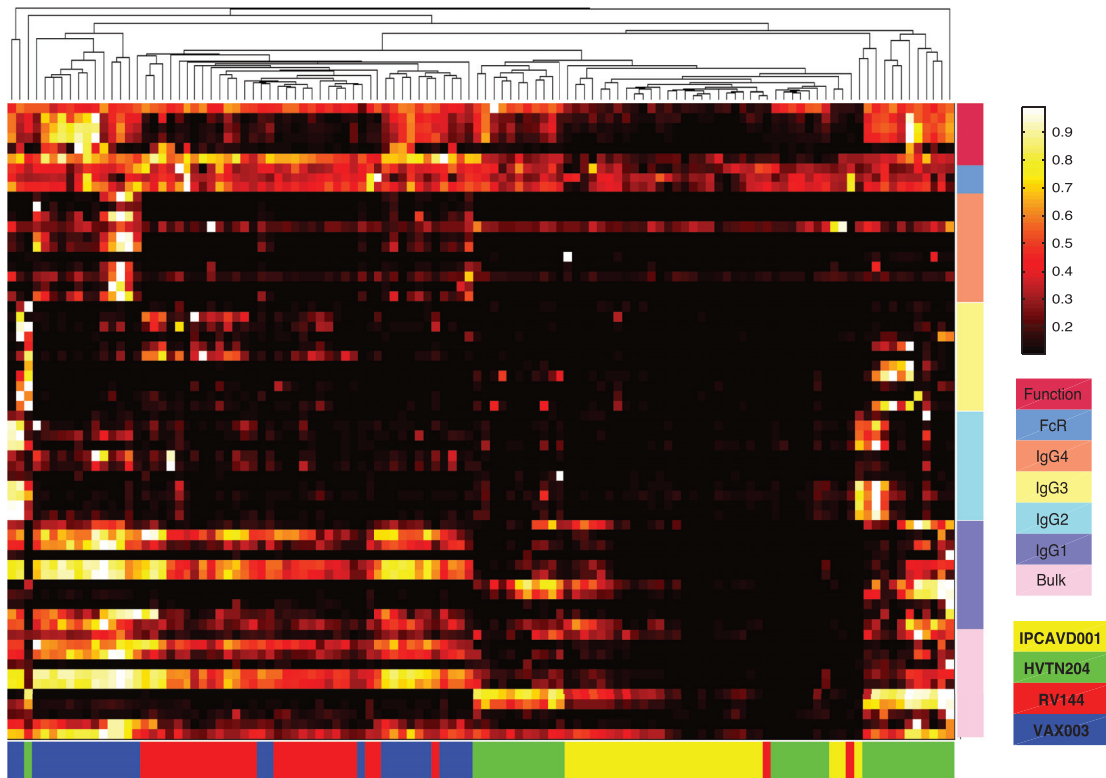
Figure 2. Hierarchical Clustering of Vaccine Trial Profiles by Biophysical Properties and Functional Responses
Data were compiled for the four different vaccine trials. Each column represents the full Ab profile of an individual subject. Colored bars along the bottom correspond to the vaccine trial for each subject. Ab properties are grouped by generalized features (Function, FcR affinity, Bulk IgG, IgG1, IgG2, IgG3, and IgG4), indicated by the colored bars on the right. Specific features are listed in Table S2.
See also Table S1.

(poxvirus prime/protein boost) samples (Figure 2, cluster 2: blue and red, respectively). While this clustering highlights the dominant influence of immunogen type in directing distinct humoral profiles, specific features driving this separation cannot be clearly discerned.

To gain enhanced resolution on the key features contributing to profile differences, a multidimensional combined feature selection method (the least absolute shrinkage and selection operator; LASSO) (Tibshirani, 1997) and partial least-squares discriminant analysis (PLSDA) (Arnold et al., 2015; Lau et al., 2011) were used. Focusing initially on RV144 and VAX003, which shared the same protein immunogen but provided different efficacies, as few as 7 of the 64 features accounted for 76% of the variance across the two trials, driving nearly complete resolution of the vaccine profiles (Figures 3A and 3B). Separation of the Ab profiles was observed in the scores plot, with points representing individual RV144 (red) or VAX003 (blue) vaccinees (Figure 3A). Differences between vaccine-elicited Ab profiles were largely captured along the first dimension (LV1), which accounted for the majority of the variance between the two trials (61%). The corresponding loadings plot (Figure 3B) illustrates the contribution of the seven LASSO features, where the relative location of an individual feature is associated with the corresponding vaccine subpopulation in the scores plot (Figure 3A). Elevated

gp120-specific IgG3 levels, relative to other features (Figure 3B), uniquely marked the RV144 vaccine profile (Figure 3A), as previously described (Chung et al., 2014b; Yates et al., 2014). By contrast, the VAX003 Ab profile was associated with known induction of higher total HIV gp140-specific Ab titers, dominated by IgG4 (Chung et al., 2014b). However, additional novel features were identified that associated with the non-protective VAX003 profile, including elevated total gp140-specific responses, higher Ab-driven NK cell degranulation, and chemokine secretion. This result suggests that differences in relationships between Ab features rather than the total Ab amount may be essential for resolving "protective" from "non-protective" vaccine profiles. Moreover, the scores plot highlights an unappreciated level of heterogeneity among the RV144 vaccinees, with respect to the magnitude of the IgG3 response, where 26% of the RV144 vaccinees exhibited a more highly skewed IgG3 response specifically across the second dimension, LV2 (Figure 3A).

When all four vaccine trials were analyzed simultaneously, 15 of the 64 features separated the vaccine profiles, accounting for 57% of the variance. The first dimension (LV1) revealed a similar separation as the hierarchical clustering analysis, separating based on protein (Figure 3C, right) versus Ad-based vectored immunization (33% variance), confirming the dominant effect of immunogen type in directing humoral profiles. LV1
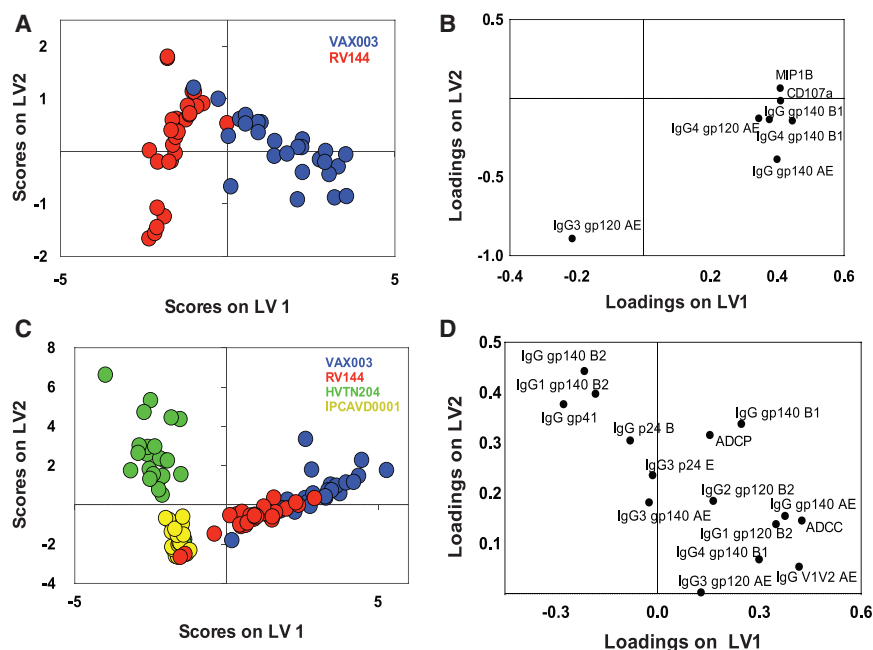
Figure 3. PLSDA and LASSO Identify Unique Combinations of Features that Differentiate Vaccine Trial Ab Profiles

(A and B) In (A), the scores plot represents the RV144 (red) and VAX003 (blue) vaccine profile distribution for each vaccinee tested (dots) from the LASSO and PLSDA. Remarkably, as few as seven Ab features, listed on the loadings plot (B), separated the vaccine profiles with 100% calibration and 97% cross-validation accuracy. LV1 captured 61% of X variance and 72% of the Y variance.

(C and D) In (C), LASSO and PLSDA of all four vaccine profiles identified 15 Ab features (D) able to discriminate between the distinct vaccine regimens (red, RV144; blue, VAX003; green, HVTN204; and yellow, IPCAVD001) with 84% cross-validation accuracy. Together, LV1 and LV2 captured 57% of the X variance and 45% of the Y variance, respectively.

See also Tables S1 and S2.

separation was strongly driven by gp41-skewed immunity, due to gp41 being included in the Ad regimens but not included in VAX003 and only partially included in RV144. Furthermore, Abs targeting clade AE Ags (gp120 and V1V2) uniquely marked RV144 and VAX003 profiles, as subjects were immunized with clade AE-derived immunogens. Thus the Ag itself, rather than the vector/immunization regimen alone, was a critical determinant influencing vaccine-induced humoral profiles.

The second dimension identified additional features that further split the vaccine profiles, accounting for an additional 24% of the variance, contributing to an unexpected grouping and separation of RV144/Ad26 and VAX003/Ad5 profiles. This separation was primarily related to differences in IgG3 subclass and V1V2 levels, which scattered in multidimensional space more closely with RV144 and Ad26 profiles (Figure 3D). Therefore, markers previously associated with reduced risk of infection in RV144 co-segregated with the experimental Ad26 vaccine trial, which used a vector similar to the ones used in regimens recently shown to protect non-human primates from infection through non-neutralizing polyfunctional Abs (Barouch et al., 2015).

Thus, use of the LASSO and PLSDA, incorporating co-variation between features, identified key variables involved in classifying vaccine regimens and provided enhanced resolution of the specific Ab features associated with differentiating vaccine profiles, objectively identifying novel correlates of Ab-mediated protection.

Correlation Networks Highlight Distinct Humoral Relationships

Next, we aimed to gain insights into relationships between features contributing to differences among vaccine-induced polyclonal profiles, adapting correlation network analysis tools commonly used in the transcriptomics field. The resulting network models revealed remarkably different Ab co-regulation interactions among the vaccine regimens, providing novel insights into the specific Ab features that may contribute to unique vaccine effector profiles.

VAX003 exhibited the most interconnected network, comprising four dense subnetworks (Figure 4A). The most prominent subnetworks included an unusual tightly tethered mixture of IgG2 and IgG3 responses that are rarely co-selected (Chaudhuri and Alt, 2004; Chaudhuri et al., 2007), pointing to the induction of a non-coherent poorly coordinated functional response (Chung et al., 2014b). Interestingly, all Fc-effector functions were connected to a third subnetwork consisting largely of IgG1 and bulk IgG responses specific for a broad array of Ags that was unexpectedly connected to the fourth IgG4 subnetwork. IgG4 Abs have previously shown to compete actively for immune complex occupancy, resulting in dampened Ab function (Chung et al., 2014b). Thus, the VAX003 network exhibited linked IgG1/IgG4 responses staggered next to a dense IgG2/IgG3 cluster, highlighting the peculiar subclass co-selection profiles driven by the non-protective VAX003 strategy.

While less prominent clusters emerged in the RV144 network model (Figure 4B), ADCP, ADCD, and ADCC were largely tethered to a network of gp120-, gp140- or V1V2-specific IgG1 and/or IgG3 responses. The V1V2B-specific IgG3 response was highly associated with the large IgG1 network, suggesting that high IgG3 V1V2B-specific responses act as a critical surrogate of a coordinated IgG3 and IgG1 response. The total IgG V1V2AE response was directly tethered to both ADCP and ADCC, suggesting that this specific V1V2 response may play an influential role in driving Ab functionality. IgG3 V1V2B and IgG3 V1V2AE responses were not directly correlated, suggesting that these V1V2 responses may represent disparate humoral immune responses rather than a single cross-reactive response. Moreover, because depletion of IgG3 only results in 30% reduction in Ab functionality (Chung et al., 2014b), it is likely that IgG3 responses may serve as a surrogate for a subpopulation
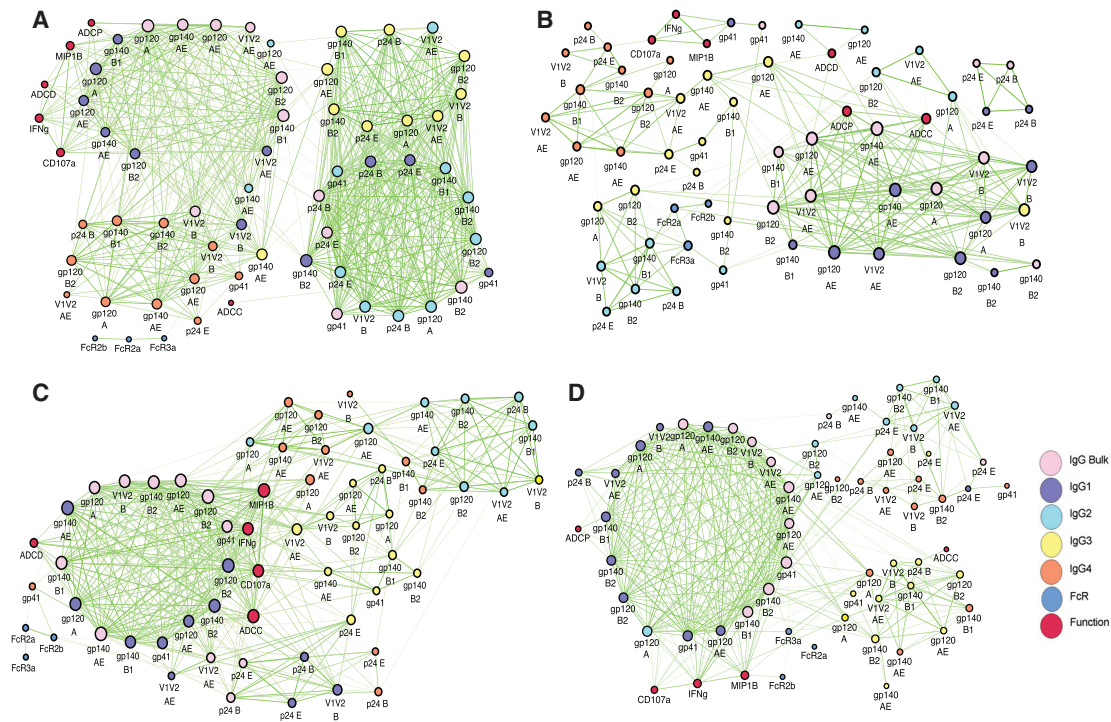
Figure 4. Correlation Networks of Vaccine-Trial-Elicited Humoral Immune Responses Probe Immune Complex Dynamics
(A–D) Correlation networks were generated for VAX003 (A), RV144 (B), HVTN204 (C), and IPCAVD001 (D). Each node (circle) represents either a biophysical feature or an effector function. Nodes are connected with an edge (line) if they are significantly correlated. The different Ab isotypes are identified by different colors as indicated. Edge thickness and color intensity of the connecting lines are directly proportional to statistical significance and edge weight, respectively (thicker and brighter network interactions represent a stronger correlation). The size of each node is directly proportional to its degree of connectedness (i.e., the number of features to which that node is connected).
See also Figure S1 and Tables S1 and S2.

of vaccine-induced IgG1 Abs that direct the polyfunctional Ab responses observed in RV144.

The HVTN204 (DNA/Ad5) network (Figure 4C) contained a highly connected subnetwork, with multiple tethers to less well-connected subnetworks of additional Ab subclasses. The dominant subnetwork consisted of IgG1 Env- and V1V2-specific responses, with ADCC, ADCD, and NK cell responses tightly intercalated within the subnetwork, sandwiched between IgG1 and IgG3 responses. However, ADCP did not appear in the network. This exclusion of ADCP suggests that Ad5 and/or DNA may preclude the induction of phagocytic Ab responses, which have been linked to protection from SIV acquisition (Barouch et al., 2013b).

Conversely, the vaccine profile induced by the experimental IPCAVD001 (Ad26) exhibited a nearly single, densely connected network tethered to Ab functions and Fc-receptor binding activity (Figure 4D). The large network consisted of a tight grid of related bulk IgG/IgG1 responses, while IgG2, IgG3, and IgG4 formed sparse external clusters, including a less functional, interconnected IgG2/IgG4 cluster (Figure 4D, top right). The clear linkages between Ab functions and IgG1 features, including an IgG1 V1V2-driven ADCP response, further supports the potential role of IgG3 as a surrogate of a highly effective, polyfunctional IgG1 response.

Overall, these statistically robust network analyses (Figure S1) point to unique relationships between all features and functions among the four vaccine trials. Identification of "desirable" Ab networks delineating specific biophysical Ab feature/function relationships that are associated with protective immunity may help identify mechanisms underlying correlates, such as the association of IgG3 and V1V2 features with reduced risk of HIV infection by RV144.

System Serology Analysis of Interactions between RV144 Surrogates of Reduced Risk of Infection

Systems Serology approaches can complement existing methods for identifying predictive mechanism(s) of protective immunity. While logistic regression involves stepwise evaluation of strongly correlated individual variables, Systems Serology approaches can additionally identify relationships between Ab features that are predictive of protection. Toward this purpose, we next examined RV144 profiles segregating with known correlates of reduced risk of infection. Thus, we dissected two Ab features (IgG/IgG3 V1V2), which were previously positively associated with reduced acquisition in the RV144 case:control analysis, in our cohort of uninfected vaccinees. Importantly, IgA levels were also included in this analysis, due to their implicated role as correlates of risk (Haynes et al., 2012). Profiles were then compared between "responders" (top 33% for each
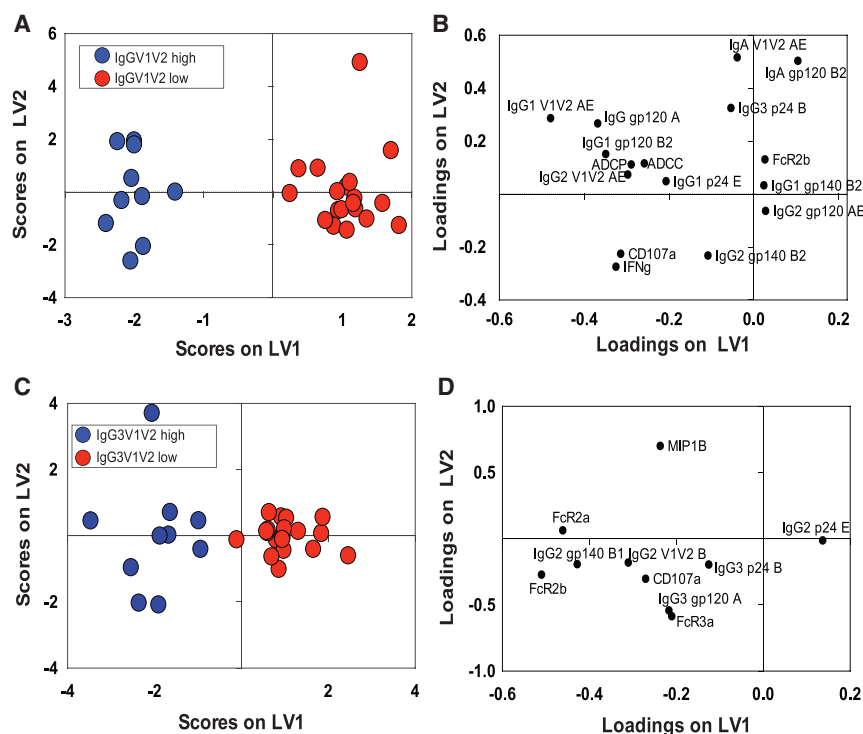
correlate of reduced risk) (Rerks-Ngarm et al., 2009; Zolla-Pazner et al., 2014) or "non-responders." The IgG V1V2 responder profile (Zolla-Pazner et al., 2014) was driven by 16 features (Figures 5A and 5B), including elevated V1V2 responses and a polyfunctional Fc-effector profile linked to higher Ab-dependent NK cell degranulation (i.e., CD107a and interferon γ [IFNγ] expression), ADCP, and ADCC. Conversely, the non-responders exhibited elevated gp120-specific IgA and increased binding to FCGR2B, the sole inhibitory Fcγ receptor, both features that have been previously associated with antagonism of Fc-effector activity (Tomaras et al., 2013; White et al., 2014).

Similar analysis of the IgG3 V1V2 correlate of reduced risk pointed to ten Ab features that distinguished responder/non-responder profiles (Figures 5C and 5D) marked by increased broad Fcγ receptor binding among responders—particularly to activating FCGR2A, involved in ADCP, and to FCGR3A, critical for NK cell degranulation and chemokine secretion. Surprisingly, IgA was not selected as a negative predictor of the IgG3 V1V2 responder profile. These findings confirm that IgG V1V2 (Figure 5A) responders exhibit a balanced polyfunctional profile, while IgG3 V1V2 responders (Figure 5B) possessed Abs selectively enhanced for binding to FCGR2A, associated with ADCP, that has been linked to protection in nonhuman primates (NHPs) (Barouch et al., 2013b).

Defining Integrative Signatures of Protective Humoral Immune Profiles in RV144

Finally, to assess whether our approach could provide enhanced resolution of mechanism(s) of potential reduced risk of infection in the RV144 trial, we next analyzed data from the case:control study (Haynes et al., 2012). Specifically, data characterizing distinct Ab subclass levels targeting multiple vaccine Ags and

functions comparable to those included in our original profiling data were included in the analysis. PLSDA using data from all cases and controls separated placebos from vaccinees, as expected, along LV1 (Figure 6A). In contrast, PLSDA of vaccinees alone was unable to separate the 40 infected from the 201 uninfected vaccinees included in the case:control analysis (Figures S2A and S2B). Similarly, network analyses showed only modest differences between vaccinated cases and controls (Figures S2C and S2D), likely related to the fact that it is unclear which uninfected vaccinees were actually exposed and protected.

To address this complication, we defined groups representing extreme profiles based on known correlates of risk (Haynes et al., 2012). Given that the IgG3 and IgG V1V2 levels were highly correlated (Figure S3), we elected to focus on the IgG V1V2 and IgA relationship due to the intriguing relationships found for these two parameters in the non-case:control data (Figure 5A). Two sets of samples were identified: (1) a region containing the greatest ratio of uninfected:infected vaccinees was classified as the "low-risk" group (Figure 6C, blue box; percentage difference = 28%, p = 0.0088), and (2) the area that contained the lowest ratio of uninfected:infected vaccinees was classified as the "risk" group (Figure 6C, red box; percentage difference = −26%, p = 0.0003). As expected, the lowest frequency of infections was observed in the IgG V1V2^high/IgA^low region of the plot, and the highest frequency of cases was observed in the IgG V1V2^low/IgA^high group. PLSDA analyses clearly separated these two groups (Figure 6D), with the low-risk group largely associated with features (Figure 6E positive loadings) that mark high IgG responses against the V1V2A scaffold as well as the V1V2-169K scaffold, corresponding to Ab responses against the viral variant able to evade the vaccine response among the infected vaccinees (Rolland et al., 2012).

Correlation networks further pointed to distinct profiles between the two groups. Three subnetworks were observed in the

low-risk case:controls—an independent small network of IgA features and two larger linked clusters, including (1) all IgG3 features and (2) IgG responses tethered to Ab functional features (Figure 6F). These two clusters contained a single link between an IgG3 response and IgG response directed at the same V1V2C scaffold, which was linked to all other V1V2 scaffold responses. Again, this suggests that the IgG3 response may be a surrogate of a highly functional IgG1 response more directly involved in modulating Ab functionality. Conversely, the risk group exhibited five clusters (Figure 6G), of which four were small groups that appeared to form relationships independent of all the IgG3 features. One of the small clusters, separate from IgG3 and all functions, included several IgG V1V2 responses, highlighting a unique structure of the humoral response among the risk group. By contrast, all IgG3 features were tightly interconnected and directly tethered to IgG features and the primary ADCC and neutralization results but not to the secondary ADCC features.

These findings indicate a mis-coordinated IgG/IgG3 V1V2 response largely separate from Ab function in the vaccinees who went on to become infected, whereas IgG/IgG3 V1V2 responses were well integrated within the network profile in vaccinees with reduced correlates of risk (i.e., IgG V1V2^{high}/IgA^{low}). Even though many of the desirable features—in particular, poly-functional responses identified in Figure 5—were not available for analysis, these data highlight the IgG V1V2 responses that likely drive protective immunity.

DISCUSSION

Because the humoral immune response consists of waves of B cell responses that progressively induce higher affinity, broadly targeting, and functionally enhanced complexes of Abs poised to eliminate a pathogen, we aimed to develop a multivariate approach that could capture the complexity of interactions between Abs at unprecedented depths. The Systems Serology approach described here not only identified features reported in previous correlates analyses, including elevated IgG3 responses in RV144 (Chung et al., 2014b; Yates et al., 2014) and Ab binding to V1V2 (Zolla-Pazner et al., 2014), but also pointed to largely indirect connections between V1V2 IgG or IgG3 responses and Ab function (ADCC, ADCP, and ADCD) in vaccinees (Figure 4B) and the low-risk RV144 case:control samples (Figure 6F). Instead, vaccine-specific IgG1 responses were largely directly tethered to Ab function (Figure 4B). This suggests that the IgG3 "protective" signatures may either represent a surrogate of an effective Ab response or only contribute in combination with multiple other Ab features (e.g., IgG1) to induce antiviral activity. Along these lines, while depletion of IgG3 Abs from RV144 vaccinees resulted in a significant loss of ADCP and ADCC activity, the activity was not completely depleted with the removal of this subclass of Abs (Chung et al., 2014b), suggesting that IgG3 Abs alone do not mediate the activity in polyclonal R144 sera and that function was also mediated by Abs remaining in the depleted purified IgGs. Therefore, the induction of IgG3 responses in RV144 may mark the coordinated production of highly functional IgG1 responses that may be functionally enhanced through altered IgG1 glycosylation, known to impact Fc-receptor affinity (Chung et al., 2014a), rather than subclass

selection differences alone (Chung et al., 2014a; Hristodorov et al., 2013). Thus, together with the IgG3 Abs, these IgG1 Abs may form highly functional immune complexes that are able to rapidly and effectively clear the virus or infected cells.

Interestingly, while vaccine-induced IgA responses were associated with enhanced risk of infection (Haynes et al., 2012), IgA emerged as an antagonist of the IgG V1V2 (Figures 5A and 5B) response but not the IgG3 response in the PLSDA analyses (Figures 5C and 5D). Furthermore, IgA responses were not connected to any of the subnetworks containing functional responses identified in the network analyses, suggesting that IgA responses may serve as a marker of a deregulated or less functional humoral immune response rather than a direct antagonist of protective humoral immune responses. Thus, while it is certain that pre-incubation of Ag with IgA monoclonal Abs may prevent IgG1 and IgG3 monoclonal Ab binding (Tomaras et al., 2013), it does not appear that these responses were directly co-induced (Figure 6). Moreover, given that the infected vaccinees exhibited both the lowest and the highest levels of IgA responses (Figure 6B), it is unlikely that IgA responses directly contributed to impaired humoral immune protection. Likewise, monoclonal therapeutics generated as IgAs exhibit potent cytotoxicity and clearance of tumor targets through Fcα receptors expressed on effector cells (e.g., neutrophils and macrophages) (Black et al., 1996; Dechant and Valerius, 2001) and have been recently linked to protection from simian-HIV (SHIV) challenge (Watkins et al., 2013). Thus, future studies may aim to define the vaccine strategies that most effectively co-select a highly functional blood IgG response and a highly effective IgA response that may collectively prevent infection at the portal of entry.

Protection from infectious diseases like HIV will likely require the targeted containment of viral replication/dissemination at the site of infection. Along these lines, HIV is transmitted across mucosal barriers, where FcγR2-expressing monocytes/macrophages are abundant (Brown and Mattapallil, 2014; Zigmond and Jung, 2013). Moreover, ADCP activity was present in the RV144, VAX003, and IPCAVD001 networks (Figure 4) but was not observed in the HVTN204 network (Figure 4C) that was highly skewed to the elicitation of NK-cell-mediated activities. Conversely, ADCP was tightly tethered within the RV144 and IPCAVD001 networks (Figure 4), was enhanced in the high V1V2 IgG3/IgG1 RV144 vaccinees (Figure 5), and was previously associated with protection in NHP (Barouch et al., 2013b). Thus these results raise the possibility that ADCP may represent a critical function, within polyfunctional Ab profiles, that is required for protection from mucosal transmission.

Beyond HIV, these vaccine-profiling approaches have broad applications and can aid in vaccine design efforts against many of the deadliest global pathogens for which immune correlates of protection have yet to be elucidated. For example, recent clinical evidence suggests that Abs present in Ebola-virus-infected convalescent immune sera contribute to improved clinical outcomes in infected patients (Kreil, 2015; Lyon et al., 2014); and, recently, vesicular stomatitis virus (VSV) vaccination has been shown to drive robust humoral immune responses (Regules et al., 2015) that provide protection from infection (Henao-Restrepo et al., 2015). However, the specific mechanism(s) by which Abs provide protection remains unclear. Yet,
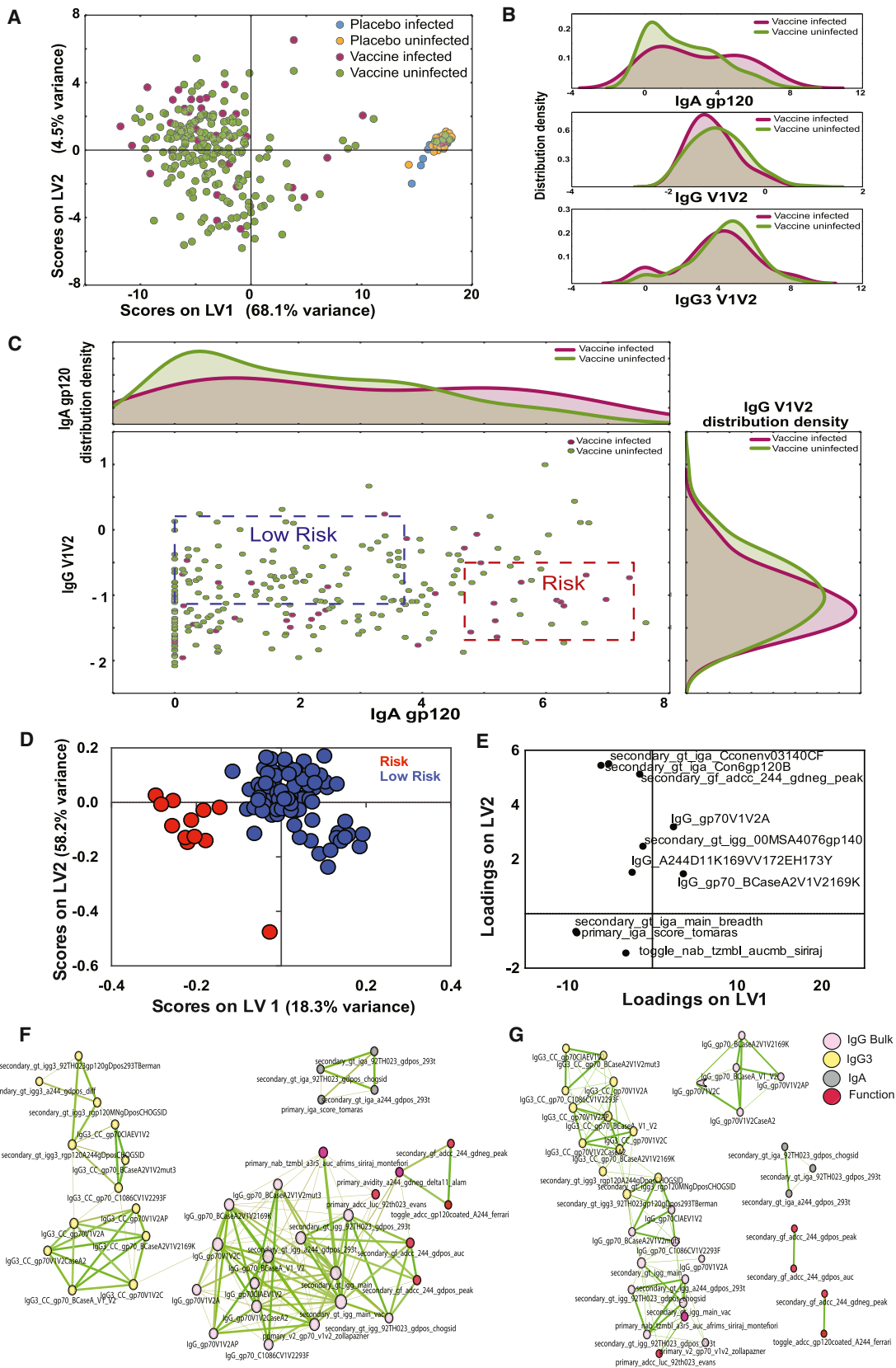
(legend on next page)

a non-neutralizing monoclonal Ab, 13c6, has been shown to provide protection from infection in an Fc-dependent manner (Olinger et al., 2012), suggesting that non-neutralizing Ab functions contribute to antiviral immunity. Thus, similar to the application of Systems Serology for the evaluation of HIV vaccine responses, the application of a Systems-Serology-guided dissection of natural humoral immune profiles that emerge in Ebola virus survivors and vaccinees may provide insights into the immunological correlates and mechanisms of protection that may help guide future vaccine efforts.

Thus, in this article, Systems Serological profiling provides a novel approach for the dissection of four HIV vaccine regimen profiles at unprecedented depths and a framework for dissecting the immune profiles that segregate with previously defined correlates of risk in efficacy studies. Systems Serology complements traditional multivariate approaches aimed at defining independent predictors of vaccine efficacy, aiding in the identification of Ab function/feature relationships that track with protective humoral immune profiles. Accordingly, these relational tools provide an additional powerful method for comparing the immune profiles of different vaccine groups/outcomes to provide greater mechanistic insights underlying the relationships of features that may contribute to immune control. While this analysis included 64 humoral features, many other features can be collected, including measures of neutralization, affinity, Fc glycosylation, and so forth. Moreover, these techniques may be expanded to examine the protective/immunopathological role of Abs in non-infectious disease settings, including malignancies and/or autoimmunity, as well as how Abs may differ among gender, ethnicity, and age. Thus, this study lays the groundwork for the evaluation, deep characterization, and comparison of polyclonal vaccine profiles for many future vaccines, for which correlates of protective immunity are still elusive.

EXPERIMENTAL PROCEDURES

Vaccine Samples
RV144 (Rerks-Ngarm et al., 2009): plasma samples from 30 vaccinated subjects at week 26 (2 weeks after the final vaccination) were provided by the Military HIV Research Program (MHRP). RV144 case:control study data were provided by the RV144 study team. Serum samples from 30 vaccinated subjects at month 30.5 (2 weeks after the final vaccination) were provided by the Global Solutions for Infectious Disease (GSID). HVTN204 (Churchyard et al., 2011): Serum samples from 30 vaccinated subjects at 2 weeks after the final vaccination were provided by the National Institute of Allergy and Infectious Diseases (NIAID) HIV Vaccine Trials Network (HVTN). IPCAVD 001 (Barouch et al., 2013a): Serum samples from 30 vaccine subjects at 2 weeks after the final

vaccination were provided by Dan Barouch. Detailed descriptions of each vaccine are included in the Supplemental Information.

Purifying Bulk IgG
IgG was purified from all vaccine plasma and serum samples using Melon Gel columns according to the manufacturer's instructions (Thermo Scientific), and the concentration was calculated using a human IgG ELISA kit (Mabtech).

Ab-Functional Profiling
The following assays were performed to functionally profile the Fc-effector functions of all vaccine Abs. In order to assess ADCP, a THP-1-based ADCP assay was performed as previously described (Ackerman et al., 2011). ADCC was assayed using a modified rapid fluorescent ADCC (RFADCC), as previously described (Gómez-Román et al., 2006); (Chung et al., 2014b). ADCD was assessed via the measurement of complement component C3b deposition on the surface of target cells. Ab-dependent NK cell degranulation and cytokine/chemokine secretion were measured using the CEM-NKr CCR5+ T-lymphoblast cell line pulsed with vaccine-specific gp120 (60 mg/ml), as previously described (Chung et al., 2014b). Detailed methods of each functional assay are described in the Supplemental Information.

Ab Biophysical Profiling
The following assays were performed to assess the biophysical profile of each of the vaccine Ab samples. Ab affinity for FCGRs was determined using surface plasmon resonance as previously described (Chung et al., 2014a), while a customized Luminex isotype assay was used to quantify the relative concentration of each Ab isotype to a panel of HIV-specific Abs. Detailed methods of each of these profiling tools are included in the Supplemental Information.

Identification of Vaccine-Specific Signatures with LASSO and PLSDA
The minimum signature of Ab features and functional parameters useful for differentiating vaccine groups were identified using the LASSO method (Tibshirani, 1997) and implemented using MATLAB software (version 2014a, MathWorks). PLSDA (Arnold et al., 2015; Lau et al., 2011) assessed the predictive ability of LASSO-selected biomarkers for classifying vaccine groups. A detailed description of validation and quality control for this analysis is included in the Supplemental Information.

Network Interactions
Networks were constructed based on the pairwise correlation coefficients between all biophysical features and functional responses. Edges between nodes are weighted using significant correlation coefficients, ρ_{ij}, after correcting for multiple comparisons (Benjamini-Hochberg q value < 0.05, testing the hypothesis of zero correlation) as follows:

$$A_{ij} = \rho_{ij}^{\alpha}$$

with $\alpha = 6$.

To assess the significance of the variable groupings observed in the network, we calculated the network clustering coefficient for the original

Figure 6. Defining Novel Signatures of Protection in the RV144 Case:Control Data
(A) The PLSDA shows the distribution of all case:control data, including all infected and uninfected placebos as well as infected and uninfected vaccinees using 101 humoral features (described in Table S3). LV1 accounted for 68.1% of all variance, separating most placebos from the vaccines, while LV2 only contributed to 4.5% of the variance.
(B) Further insights into the distribution of IgA gp120, IgG V1V2, and IgG3 V1V2 levels were analyzed using histograms demonstrating unique multi-modal differences in feature distribution among the infected and uninfected vaccinees.
(C) The scatterplot, in the central panel, represents the bivariate distribution of IgA gp120 and IgG V1V2 in the vaccines and is framed by the histogram distributions for unidimensional reference. The blue and red dash-lined boxes represent quadrants within the data that constitute the fewest cases:controls (low risk, blue) or the highest ratio of cases:controls (high risk, red).
(D and E) LASSO and PLSDA identified nine features that split low- and high-risk profile separation with 97.8% accuracy in cross-validation. Together, LV1 and LV2 captured 70.4% of the X variance and 30.1% of the Y variance, respectively.
(F and G) Correlation networks were generated for both the low-risk (F) and high-risk (G) groups.
See also Figures S2 and S3 and Table S3.

network and for 100 randomized networks. Random networks are generated by randomly swapping edges while preserving the degree of all nodes (degree-preserving edge shuffle) (Figure S2).

RV144 Case:Control Study Data Processing

RV144 case:control study data included results from 281 patients, including 101 Ab features and functional parameters. Specific features used within this analysis are documented in Table S3. Subjects were categorized into four groups including: placebo infected, placebo uninfected, vaccine infected, and vaccine uninfected for all analyses. Because IgG3 and IgG V1V2 levels were highly correlated (Figure S3), vaccinees were classified based on their IgG V1V2 and IgA levels. A high-risk or low-risk group was defined as the region of the IgG V1V2 versus IgA plot that contained the fewest cases or the fewest controls, respectively, in a mutually exclusive manner. The percentage difference between infected versus uninfected vaccinees was defined as

$$P = \left(\frac{I_r}{I_t} - \frac{U_r}{U_t} \right) \times 100,$$

where, for any given region, r, the percentage of infected people, I_r, over the infected population, I_t, was calculated, as well as for uninfected individuals. The enriched region, with the highest P was defined as the high-risk group, whereas the region with the lowest P was defined as the low-risk group. Fisher's exact test was used to estimate the significance of the enriched region from a null hypothesis.

SUPPLEMENTAL INFORMATION

Supplemental Information includes Supplemental Experimental Procedures, three figures, and three tables and can be found with this article online at http://dx.doi.org/10.1016/j.cell.2015.10.027.

AUTHOR CONTRIBUTIONS

ACKNOWLEDGMENTS

REFERENCES

Ackerman, M.E., and Alter, G. (2013). Opportunities to exploit non-neutralizing HIV-specific antibody activity. Curr. HIV Res. *11*, 365–377.

Ackerman, M.E., Moldt, B., Wyatt, R.T., Dugast, A.S., McAndrew, E., Tsoukas, S., Jost, S., Berger, C.T., Sciaranghella, G., Liu, Q., et al. (2011). A robust, high-throughput assay to determine the phagocytic activity of clinical antibody samples. J. Immunol. Methods *366*, 8–19.

Arnold, K.B., Burgener, A., Birse, K., Romas, L., Dunphy, L.J., Shahabi, K., Abou, M., Westmacott, G.R., McCorrister, S., Kwatampora, J., et al. (2015). Increased levels of inflammatory cytokines in the female reproductive tract are associated with altered expression of proteases, mucosal barrier proteins, and an influx of HIV-susceptible target cells. Mucosal Immunol. Published online June 24, 2015. http://dx.doi.org/10.1038/mi.2015.51.

Barouch, D.H., Liu, J., Peter, L., Abbink, P., Iampietro, M.J., Cheung, A., Alter, G., Chung, A., Dugast, A.S., Frahm, N., et al. (2013a). Characterization of humoral and cellular immune responses elicited by a recombinant adenovirus serotype 26 HIV-1 Env vaccine in healthy adults (IPCAVD 001). J. Infect. Dis. *207*, 248–256.

Barouch, D.H., Stephenson, K.E., Borducchi, E.N., Smith, K., Stanley, K., McNally, A.G., Liu, J., Abbink, P., Maxfield, L.F., Seaman, M.S., et al. (2013b). Protective efficacy of a global HIV-1 mosaic vaccine against heterologous SHIV challenges in rhesus monkeys. Cell *155*, 531–539.

Barouch, D.H., Alter, G., Broge, T., Linde, C., Ackerman, M.E., Brown, E.P., Borducchi, E.N., Smith, K.M., Nkolola, J.P., Liu, J., et al. (2015). HIV-1 vaccines. Protective efficacy of adenovirus/protein vaccines against SIV challenges in rhesus monkeys. Science *349*, 320–324.

Black, K.P., Cummins, J.E., Jr., and Jackson, S. (1996). Serum and secretory IgA from HIV-infected individuals mediate antibody-dependent cellular cytotoxicity. Clin. Immunol. Immunopathol. *81*, 182–190.

Bournazos, S., Klein, F., Pietzsch, J., Seaman, M.S., Nussenzweig, M.C., and Ravetch, J.V. (2014). Broadly neutralizing anti-HIV-1 antibodies require Fc effector functions for in vivo activity. Cell *158*, 1243–1253.

Brown, D., and Mattapallil, J.J. (2014). Gastrointestinal tract and the mucosal macrophage reservoir in HIV infection. Clin. Vaccine Immunol. *21*, 1469–1473.

Chaudhuri, J., and Alt, F.W. (2004). Class-switch recombination: interplay of transcription, DNA deamination and DNA repair. Nat. Rev. Immunol. *4*, 541–552.

Chaudhuri, J., Basu, U., Zarrin, A., Yan, C., Franco, S., Perlot, T., Vuong, B., Wang, J., Phan, R.T., Datta, A., et al. (2007). Evolution of the immunoglobulin heavy chain class switch recombination mechanism. Adv. Immunol. *94*, 157–214.

Chung, A.W., and Alter, G. (2014). Dissecting the antibody constant region protective immune parameters in HIV infection. Future Virol. *9*, 397–414.

Chung, A.W., Crispin, M., Pritchard, L., Robinson, H., Gorny, M.K., Yu, X., Bailey-Kellogg, C., Ackerman, M.E., Scanlan, C., Zolla-Pazner, S., and Alter, G. (2014a). Identification of antibody glycosylation structures that predict monoclonal antibody Fc-effector function. AIDS *28*, 2523–2530.

Chung, A.W., Ghebremichael, M., Robinson, H., Brown, E., Choi, I., Lane, S., Dugast, A.S., Schoen, M.K., Rolland, M., Suscovich, T.J., et al. (2014b). Polyfunctional Fc-effector profiles mediated by IgG subclass selection distinguish RV144 and VAX003 vaccines. Sci. Transl. Med. *6*, 228ra38.

Churchyard, G.J., Morgan, C., Adams, E., Hural, J., Graham, B.S., Moodie, Z., Grove, D., Gray, G., Bekker, L.G., McElrath, M.J., et al.; NIAID HIV Vaccine Trials Network (2011). A phase IIA randomized clinical trial of a multiclade HIV-1 DNA prime followed by a multiclade rAd5 HIV-1 vaccine boost in healthy adults (HVTN204). PLoS ONE *6*, e21225.

Dechant, M., and Valerius, T. (2001). IgA antibodies for cancer therapy. Crit. Rev. Oncol. Hematol. *39*, 69–77.

DiLillo, D.J., Tan, G.S., Palese, P., and Ravetch, J.V. (2014). Broadly neutralizing hemagglutinin stalk-specific antibodies require FcγR interactions for protection against influenza virus in vivo. Nat. Med. *20*, 143–151.

Gómez-Román, V.R., Florese, R.H., Patterson, L.J., Peng, B., Venzon, D., Aldrich, K., and Robert-Guroff, M. (2006). A simplified method for the rapid fluorometric assessment of antibody-dependent cell-mediated cytotoxicity. J. Immunol. Methods *308*, 53–67.

Haynes, B.F., Gilbert, P.B., McElrath, M.J., Zolla-Pazner, S., Tomaras, G.D., Alam, S.M., Evans, D.T., Montefiori, D.C., Karnasuta, C., Sutthent, R., et al. (2012). Immune-correlates analysis of an HIV-1 vaccine efficacy trial. N. Engl. J. Med. *366*, 1275–1286.

Henao-Restrepo, A.M., Longini, I.M., Egger, M., Dean, N.E., Edmunds, W.J., Camacho, A., Carroll, M.W., Doumbia, M., Draguez, B., Duraffour, S., et al. (2015). Efficacy and effectiveness of an rVSV-vectored vaccine expressing Ebola surface glycoprotein: interim results from the Guinea ring vaccination cluster-randomised trial. Lancet *386*, 857–866.

Hessell, A.J., Hangartner, L., Hunter, M., Havenith, C.E., Beurskens, F.J., Bakker, J.M., Lanigan, C.M., Landucci, G., Forthal, D.N., Parren, P.W., et al. (2007). Fc receptor but not complement binding is important in antibody protection against HIV. Nature *449*, 101–104.

Hristodorov, D., Fischer, R., and Linden, L. (2013). With or without sugar? (A) glycosylation of therapeutic antibodies. Mol. Biotechnol. *54*, 1056–1068.

Jegerlehner, A., Schmitz, N., Storni, T., and Bachmann, M.F. (2004). Influenza A vaccine based on the extracellular domain of M2: weak protection mediated via antibody-dependent NK cell activity. J. Immunol. *172*, 5598–5605.

Joos, C., Marrama, L., Polson, H.E., Corre, S., Diatta, A.M., Diouf, B., Trape, J.F., Tall, A., Longacre, S., and Perraut, R. (2010). Clinical protection from falciparum malaria correlates with neutrophil respiratory bursts induced by merozoites opsonized with human serum antibodies. PLoS ONE *5*, e9871.

Kohl, S., and Loo, L.S. (1982). Protection of neonatal mice against herpes simplex virus infection: probable in vivo antibody-dependent cellular cytotoxicity. J. Immunol. *129*, 370–376.

Kohl, S., Loo, L.S., and Pickering, L.K. (1981). Protection of neonatal mice against herpes simplex viral infection by human antibody and leukocytes from adult, but not neonatal humans. J. Immunol. *127*, 1273–1275.

Kreil, T.R. (2015). Treatment of Ebola virus infection with antibodies from reconvalescent donors. Emerg. Infect. Dis. *21*, 521–523.

Lau, K.S., Juchheim, A.M., Cavaliere, K.R., Philips, S.R., Lauffenburger, D.A., and Haigis, K.M. (2011). In vivo systems analysis identifies spatial and temporal aspects of the modulation of TNF-α-induced apoptosis and proliferation by MAPKs. Sci. Signal. *4*, ra16.

Lyon, G.M., Mehta, A.K., Varkey, J.B., Brantly, K., Plyler, L., McElroy, A.K., Kraft, C.S., Towner, J.S., Spiropoulou, C., Ströher, U., et al.; Emory Serious Communicable Diseases Unit (2014). Clinical care of two patients with Ebola virus disease in the United States. N. Engl. J. Med. *371*, 2402–2409.

Olinger, G.G., Jr., Pettitt, J., Kim, D., Working, C., Bohorov, O., Bratcher, B., Hiatt, E., Hume, S.D., Johnson, A.K., Morton, J., et al. (2012). Delayed treatment of Ebola virus infection with plant-derived monoclonal antibodies provides protection in rhesus macaques. Proc. Natl. Acad. Sci. USA *109*, 18030–18035.

Osier, F.H., Feng, G., Boyle, M.J., Langer, C., Zhou, J., Richards, J.S., McCallum, F.J., Reiling, L., Jaworowski, A., Anders, R.F., et al. (2014). Opsonic phagocytosis of Plasmodium falciparum merozoites: mechanism in human immunity and a correlate of protection against malaria. BMC Med. *12*, 108.

Pitisuttithum, P., Gilbert, P., Gurwith, M., Heyward, W., Martin, M., van Griensven, F., Hu, D., Tappero, J.W., and Choopanya, K.; Bangkok Vaccine Evaluation Group (2006). Randomized, double-blind, placebo-controlled efficacy trial of a bivalent recombinant glycoprotein 120 HIV-1 vaccine among injection drug users in Bangkok, Thailand. J. Infect. Dis. *194*, 1661–1671.

Pulendran, B., and Ahmed, R. (2011). Immunological mechanisms of vaccination. Nat. Immunol. *12*, 509–517.

Regules, J.A., Beigel, J.H., Paolino, K.M., Voell, J., Castellano, A.R., Muñoz, P., Moon, J.E., Ruck, R.C., Bennett, J.W., Twomey, P.S., et al.; rVSVΔG-ZEBOV-GP Study Group (2015). A recombinant vesicular stomatitis virus Ebola vaccine—preliminary report. N. Engl. J. Med. Published online April 1, 2015. http://dx.doi.org/10.1056/NEJMoa1414216.

Rerks-Ngarm, S., Pitisuttithum, P., Nitayaphan, S., Kaewkungwal, J., Chiu, J., Paris, R., Premsri, N., Namwat, C., de Souza, M., Adams, E., et al.; MOPH-TAVEG Investigators (2009). Vaccination with ALVAC and AIDSVAX to prevent HIV-1 infection in Thailand. N. Engl. J. Med. *361*, 2209–2220.

Rolland, M., Edlefsen, P.T., Larsen, B.B., Tovanabutra, S., Sanders-Buell, E., Hertz, T., deCamp, A.C., Carrico, C., Menis, S., Magaret, C.A., et al. (2012). Increased HIV-1 vaccine efficacy against viruses with genetic signatures in Env V2. Nature *490*, 417–420.

Tibshirani, R. (1997). The lasso method for variable selection in the Cox model. Stat. Med. *16*, 385–395.

Tomaras, G.D., Ferrari, G., Shen, X., Alam, S.M., Liao, H.X., Pollara, J., Bonsignori, M., Moody, M.A., Fong, Y., Chen, X., et al. (2013). Vaccine-induced plasma IgA specific for the C1 region of the HIV-1 envelope blocks binding and effector function of IgG. Proc. Natl. Acad. Sci. USA *110*, 9019–9024.

Warfield, K.L., Swenson, D.L., Olinger, G.G., Kalina, W.V., Aman, M.J., and Bavari, S. (2007). Ebola virus-like particle-based vaccine protects nonhuman primates against lethal Ebola virus challenge. J. Infect. Dis. *196* (*Suppl 2*), S430–S437.

Watkins, J.D., Sholukh, A.M., Mukhtar, M.M., Siddappa, N.B., Lakhashe, S.K., Kim, M., Reinherz, E.L., Gupta, S., Forthal, D.N., Sattentau, Q.J., et al.; CAVD Project Group (2013). Anti-HIV IgA isotypes: differential virion capture and inhibition of transcytosis are linked to prevention of mucosal R5 SHIV transmission. AIDS *27*, F13–F20.

White, A.L., Beers, S.A., and Cragg, M.S. (2014). FcγRIIB as a key determinant of agonistic antibody efficacy. Curr. Top. Microbiol. Immunol. *382*, 355–372.

Yates, N.L., Liao, H.X., Fong, Y., deCamp, A., Vandergrift, N.A., Williams, W.T., Alam, S.M., Ferrari, G., Yang, Z.Y., Seaton, K.E., et al. (2014). Vaccine-induced Env V1-V2 IgG3 correlates with lower HIV-1 infection risk and declines soon after vaccination. Sci. Transl. Med. *6*, 228ra39.

Zigmond, E., and Jung, S. (2013). Intestinal macrophages: well educated exceptions from the rule. Trends Immunol. *34*, 162–168.

Zolla-Pazner, S., deCamp, A., Gilbert, P.B., Williams, C., Yates, N.L., Williams, W.T., Howington, R., Fong, Y., Morris, D.E., Soderberg, K.A., et al. (2014). Vaccine-induced IgG antibodies to V1V2 regions of multiple HIV-1 subtypes correlate with decreased risk of HIV-1 infection. PLoS ONE *9*, e87572.